

Frequentist perspective on robust parameter estimation using the ensemble Kalman filter

Sebastian Reich¹

University of Potsdam, Institute of Mathematics, Potsdam, Germany
sebastian.reich@uni-postdam.de,

Abstract. Standard maximum likelihood or Bayesian approaches to parameter estimation of stochastic differential equations are not robust to perturbations in the continuous-in-time data. In this note, we give a rather elementary explanation of this observation in the context of continuous-time parameter estimation using an ensemble Kalman filter. We employ the frequentist perspective to shed new light on two robust estimation techniques; namely subsampling the data and rough path corrections. We illustrate our findings through a simple numerical experiment.

Keywords: parameter estimation, stochastic differential equations, ensemble Kalman filter, frequentist approach, rough path theory

1 Introduction

In this note, we revisit the well-studied problem of parameter estimation for stochastic differential equations (SDEs) [23]. Our particular perspective is driven by online (time-continuous) state and parameter estimation [6, 10] using the popular ensemble Kalman filter (EnKF) and its continuous-time ensemble Kalman-Bucy filter (EnKBF) formulations [14, 9, 24]. As for the corresponding maximum likelihood approaches [25, 13] and as detailed in [8] using rough path theory [15], it turns out that the EnKBF is not robust with respect to continuous perturbations in the data; a fact that is also well-known for SDEs subject to multiplicative noise [21]. Here we expand on this observation by a frequentist analysis of the EnKBF estimators in the spirit of [27]. In order to facilitate a rather elementary mathematical analysis, we consider the very much simplified problem of parameter estimation for linear SDEs only. This restriction allows us to avoid certain technicalities from rough path theory and enables a rather straightforward application of the numerical rough path approach put forward in [12]. As a result we are able to demonstrate that the popular approach of subsampling the data [2, 25, 5] can be well justified from a frequentist perspective. The frequentist perspective also suggests a rather natural approach to the estimation of the required correction term in case an EnKBF is implemented without subsampling. We end this introductory paragraph with a reference to [1], which includes a broad survey on alternative estimation techniques. We also point to [8] for a

more in-depth discussion of rough path theory in connection with filtering and parameter estimation.

The remainder of this note is structured as follows. The problem setting and the EnKBF are introduced in the subsequent Section 2. The frequentist perspective and its implications on the specific implementations of an EnKBF in the context of low and high frequency data assimilation are laid out in Section 3. The importance of these considerations becomes transparent when applying the EnKBF to perturbed data in Section 4. Here again, we restrict to a rather simple model setting taken from [16] and also used in [8]. As a result we build a clear connection between subsampling and the necessity for a correction term in case high frequency data is assimilated directly. A brief numerical demonstration is provided in Section 5, which is followed by a concluding remark in Section 6.

2 Ensemble Kalman parameter estimation

We consider the SDE parameter estimation problem

$$dX_t = f(X_t, \theta)dt + \gamma^{1/2}dW_t \quad (1)$$

subject to observations X_t^\dagger , $t \in [0, T]$, which arise from the reference system

$$dX_t^\dagger = f^\dagger(X_t^\dagger)dt + \gamma^{1/2}dW_t^\dagger, \quad (2)$$

where the unknown drift function $f^\dagger(x)$ typically satisfies $f^\dagger(x) = f(x, \theta^\dagger)$ and θ^\dagger denotes the true parameter value. Here we assume for simplicity that the unknown parameter is scalar-valued and that the state variable is d -dimensional with $d \geq 1$. Furthermore, W_t and W_t^\dagger denote independent standard d -dimensional Brownian motions and $\gamma > 0$ is the (known) diffusion constant.

Following the Bayesian paradigm, we treat the unknown parameter as a random variable Θ . Furthermore, we apply a sequential approach and update Θ with the incoming data X_t^\dagger as a function of time. The update itself is achieved by an application of the (deterministic) ensemble Kalman–Bucy filter (EnKBF) mean-field equations [9, 24], which take the form

$$d\Theta_t = \gamma^{-1}\pi_t \left[(\theta - \pi_t[\theta]) \otimes f(X_t^\dagger, \theta) \right] dI_t, \quad (3a)$$

$$dI_t = dX_t^\dagger - \frac{1}{2} \left(f(X_t^\dagger, \Theta_t) + \pi_t[f(X_t^\dagger, \theta)] \right) dt, \quad (3b)$$

where π_t denotes the probability density function (PDF) of Θ_t and $\pi_t[g]$ the associated expectation value of a function $g(\theta)$. The variable I_t , defined by (3b), is called the innovation. The initial condition $\Theta_0 \sim \pi_0$ is provided by the prior PDF of the unknown parameter.

We note in passing that there is also a stochastic variant of the innovation process [24] defined by

$$dI_t = dX_t^\dagger - f(X_t^\dagger, \Theta_t)dt - \gamma^{1/2}dW_t. \quad (4)$$

We now state a numerical implementation with step-size $\Delta t > 0$ and denote the resulting numerical approximations at $t_n = n\Delta t$ by $\Theta_n \sim \pi_n$, $n \geq 1$. The discrete-time mean-field formulation of the EnKBF

$$\Theta_{n+1} = \Theta_n + K_n \left\{ (X_{t_{n+1}}^\dagger - X_{t_n}^\dagger) - \frac{1}{2} \left(f(X_{t_n}^\dagger, \Theta_n) + \pi_n[f(X_{t_n}^\dagger, \theta)] \right) \Delta t \right\} \quad (5)$$

is inspired by [3] with Kalman gain

$$K_n = \pi_n \left[(\theta - \pi_n[\theta]) \otimes f(X_{t_n}^\dagger, \theta) \right] \times \quad (6a)$$

$$\left(\gamma + \Delta t \pi_n \left[\left(f(X_{t_n}^\dagger, \theta) - \pi_n[f(X_{t_n}^\dagger, \theta)] \right) \otimes f(X_{t_n}^\dagger, \theta) \right] \right)^{-1}. \quad (6b)$$

Remark 1. The rough path analysis of the EnKBF presented in [8] is based on a Stratonovich reformulation of (3) and its appropriate time discretisation. Here we follow the Itô/Euler–Maruyama formulation of the data-driven term in (3), that is,

$$\int_0^T g(X_t^\dagger, t) dX_t^\dagger = \lim_{\Delta t \rightarrow 0} \sum_{i=1}^L g(X_{t_n}^\dagger, t_n) (X_{t_{n+1}}^\dagger - X_{t_n}^\dagger) \quad (7)$$

for any continuous function $g(x, t)$ and $\Delta t = T/L$, as it corresponds to standard implementation of the EnKBF and is easier to analyse in the context of this paper.

The EnKBF only provides an approximate solution to the Bayesian inference problem for general nonlinear $f(x, \theta)$. However, it becomes exact in the mean-field limit for affine drift functions $f(x, \theta) = \theta Ax + Bx + c$.

Example 1. Consider the partial differential equation

$$\partial_t u = -U \partial_y u + \rho \partial_y^2 u + \dot{W} \quad (8)$$

over a periodic spatial domain $y \in [0, L)$, where $\mathcal{W}(t, y)$ denotes space-time white noise and $U \in \mathbb{R}$ as well as $\rho > 0$ are given parameters. A standard finite-difference discretisation in space with d grid points and mesh-size Δy leads to a linear system of SDEs of the form

$$d\mathbf{u}_t = -(UD + \rho DD^T) \mathbf{u}_t dt + \Delta y^{-1/2} dW_t, \quad (9)$$

where $\mathbf{u}_t \in \mathbb{R}^d$ denotes the vector of grid approximations at time t , $D \in \mathbb{R}^{d \times d}$ a finite difference approximation of the spatial derivative ∂_y , and W_t standard d -dimensional Brownian motion. We can now set $x = \mathbf{u}$, $\gamma = \Delta y^{-1}$ and identify either $\theta = U$ or $\theta = \rho$ as the unknown parameter in order to obtain a SDE of the form (1).

In this note, we further simplify our given inference problem to the case

$$f(x, \theta) = \theta Ax, \quad (10)$$

where $A \in \mathbb{R}^{d \times d}$ is a normal matrix with its eigenvalues in the left half plane, that is, $\sigma(A) \subset \mathbb{C}_-$. The reference parameter value is set to $\theta^\dagger = 1$. Hence the SDE (2) possesses a Gaussian invariant measure with mean zero and covariance matrix

$$C = -\gamma(A + A^T)^{-1}. \quad (11)$$

We assume from now on that the observations X_t^\dagger are realisations of (2) with initial condition $X_0^\dagger \sim N(0, C)$.

Under these assumptions, the EnKBF (3) simplifies drastically and we obtain

$$d\Theta_t = \frac{\sigma_t}{\gamma} (AX_t^\dagger)^T dI_t, \quad (12a)$$

$$dI_t = dX_t^\dagger - \frac{1}{2} (\Theta_t + \pi_t[\theta]) AX_t^\dagger dt, \quad (12b)$$

with variance

$$\sigma_t = \pi_t [(\theta - \pi_t[\theta])^2]. \quad (13)$$

Similarly, the discrete-time mean-field EnKF (5) reduces to

$$\Theta_{n+1} = \Theta_n + K_n \left\{ (X_{t_{n+1}}^\dagger - X_{t_n}^\dagger) - \frac{1}{2} (\Theta_n + \pi_n[\theta]) AX_{t_n}^\dagger \Delta t \right\} \quad (14)$$

with Kalman gain

$$K_n = \sigma_n (AX_{t_n}^\dagger)^T \left(\gamma + \Delta t \sigma_n (AX_{t_n}^\dagger)^T AX_{t_n}^\dagger \right)^{-1}. \quad (15)$$

Please note that

$$K_n = \frac{\sigma_n}{\gamma} (AX_{t_n}^\dagger)^T + \mathcal{O}(\Delta t). \quad (16)$$

Furthermore, since $X_t^\dagger \sim N(0, C)$,

$$(AX_t^\dagger)^T AX_t^\dagger = (A^T A) : (X_t^\dagger \otimes X_t^\dagger) \approx (A^T A) : C \quad (17)$$

for $d \gg 1$ and we may simplify the Kalman gain further to

$$K_n = \sigma_n (AX_{t_n}^\dagger)^T (\gamma + \Delta t \sigma_n (A^T A) : C)^{-1}. \quad (18)$$

The approximation (17) becomes exact in the limit $d \rightarrow \infty$, which we will frequently assume in the following section. Here we have used the notation $A : B = \text{tr}(A^T B)$ to denote the Frobenius inner product of two matrices $A, B \in \mathbb{R}^{d \times d}$.

Remark 2. The Stratonovich reformulation of (12) replaces (12a) by

$$d\Theta_t = \frac{\sigma_t}{\gamma} \left\{ (AX_t^\dagger)^T \circ dI_t - \frac{\gamma}{2} \text{tr}(A) dt \right\}. \quad (19)$$

The innovation I_t remains as before. See Appendix B of [8] for more details. An appropriate time discretisation of the innovation-driven term replace the Kalman gain (15) by

$$K_{n+1/2} = \sigma_n (AX_{t_{n+1/2}}^\dagger)^\top \left(\gamma + \Delta t \sigma_n (AX_{t_{n+1/2}}^\dagger)^\top AX_{t_{n+1/2}}^\dagger \right)^{-1}, \quad (20)$$

where

$$X_{t_{n+1/2}}^\dagger = \frac{1}{2} (X_{t_n}^\dagger + X_{t_{n+1}}^\dagger). \quad (21)$$

Please note that a midpoint discretisation of the data-driven term in (19) results in

$$(AX_{t_{n+1/2}}^\dagger)^\top (X_{t_{n+1}}^\dagger - X_{t_n}^\dagger) = (AX_{t_n}^\dagger)^\top (X_{t_{n+1}}^\dagger - X_{t_n}^\dagger) + \quad (22a)$$

$$\frac{1}{2} A^\top : (X_{t_{n+1}}^\dagger - X_{t_n}^\dagger) \otimes (X_{t_{n+1}}^\dagger - X_{t_n}^\dagger) \quad (22b)$$

and that

$$\frac{1}{2} A^\top : (X_{t_{n+1}}^\dagger - X_{t_n}^\dagger) \otimes (X_{t_{n+1}}^\dagger - X_{t_n}^\dagger) \approx \frac{\Delta t \gamma}{2} \text{tr}(A), \quad (23)$$

which justifies the additional drift term in (19). A precise meaning of the approximation in (23) will be given in Remark 3 below.

Alternatively, if one wishes to explicitly utilise the availability of continuous-time data X_t^\dagger , one could apply the following variant of (14):

$$\Theta_{n+1} = \Theta_n + \frac{\sigma_n}{\gamma} \int_{t_n}^{t_{n+1}} (AX_t^\dagger)^\top dX_t^\dagger - \frac{1}{2} K_n AX_{t_n}^\dagger (\Theta_n + \pi_n[\theta]) \Delta t \quad (24)$$

and, following the Itô/Euler–Maruyama approximation (7), discretise the integral with a small inner step-size $\Delta\tau = \Delta t/L$, $L \gg 1$; that is,

$$\int_{t_n}^{t_{n+1}} (AX_t^\dagger)^\top dX_t^\dagger \approx \sum_{l=0}^{L-1} (AX_{\tau_l}^\dagger)^\top (X_{\tau_{l+1}}^\dagger - X_{\tau_l}^\dagger) \quad (25)$$

with $\tau_l = t_n + l\Delta\tau$. We note that

$$\sum_{l=0}^{L-1} (AX_{\tau_l}^\dagger)^\top (X_{\tau_{l+1}}^\dagger - X_{\tau_l}^\dagger) = (AX_{t_n}^\dagger)^\top (X_{t_{n+1}}^\dagger - X_{t_n}^\dagger) + \quad (26a)$$

$$A^\top : \left(\sum_{l=0}^{L-1} (X_{\tau_l}^\dagger - X_{t_n}^\dagger) \otimes (X_{\tau_{l+1}}^\dagger - X_{\tau_l}^\dagger) \right) \quad (26b)$$

which is at the heart of rough path analysis [12] and which we utilise in the following section.

3 Frequentist analysis

We analyse (12) further under the assumptions that Θ_0 is Gaussian distributed with given prior mean m_{prior} and variance σ_{prior} . The conditional mean $\mu_t = \pi_t[\theta]$ satisfies the SDE

$$d\mu_t = \frac{\sigma_t}{\gamma} \left((AX_t^\dagger)^\top dX_t^\dagger - \mu_t (A^\top A) : (X_t^\dagger \otimes X_t^\dagger) dt \right), \quad (27)$$

which simplifies to

$$d\mu_t = \frac{\sigma_t}{\gamma} \left((AX_t^\dagger)^\top dX_t^\dagger - \mu_t (A^\top A) : C dt \right), \quad (28)$$

under the approximation (17). The initial condition is $\mu_0 = m_{\text{prior}}$. The evolution equation for the variance is given by

$$\frac{d}{dt}\sigma_t = -\frac{\sigma_t^2}{\gamma} (A^\top A) : (X_t^\dagger \otimes X_t^\dagger) \quad (29)$$

with initial condition $\sigma_0 = \sigma_{\text{prior}}$ and which again reduces to

$$\frac{d}{dt}\sigma_t = -\frac{\sigma_t^2}{\gamma} (A^\top A) : C \quad (30)$$

under the approximation (17).

We now perform a frequentist analysis of the estimator μ_t defined by (28) and (30) [27]. In a first step, we take the expectation of (28) over all realisations X_t^\dagger of the SDE (2), which we denote by

$$m_t := \mathbb{E}^\dagger[\mu_t]. \quad (31)$$

The associated evolution equation is given by

$$\frac{d}{dt}m_t = \frac{\sigma_t}{\gamma} (A^\top A) : \mathbb{E}^\dagger[X_t^\dagger \otimes X_t^\dagger] - \frac{\sigma_t}{\gamma} (A^\top A) : C m_t, \quad (32a)$$

which reduces to

$$\frac{d}{dt}m_t = \frac{\sigma_t}{\gamma} (A^\top A) : C (1 - m_t) = \sigma_t (A^\top A) : (A + A^\top)^{-1} (1 - m_t). \quad (33)$$

In a second step, we also look at the frequentist variance

$$p_t := \mathbb{E}^\dagger[(\mu_t - m_t)^2]. \quad (34)$$

Using

$$d(\mu_t - m_t) = \frac{\sigma_t}{\gamma} \left\{ (A^\top A) : (X_t^\dagger \otimes X_t^\dagger - C) dt + \gamma^{1/2} (AX_t^\dagger)^\top dW_t^\dagger \right\} \quad (35a)$$

$$\frac{\sigma_t}{\gamma} (A^\top A) : C (\mu_t - m_t) dt, \quad (35b)$$

we obtain

$$\frac{d}{dt}p_t = -\frac{\sigma_t}{\gamma} (A^T A) : C (2p_t - \sigma_t) + \quad (36a)$$

$$\frac{2\sigma_t}{\gamma} (A^T A) : \mathbb{E}^\dagger \left[(X_t^\dagger \otimes X_t^\dagger - C) (\mu_t - m_t) \right], \quad (36b)$$

which we simplify to

$$\frac{d}{dt}p_t = \frac{\sigma_t}{\gamma} (A^T A) : C (\sigma_t - 2p_t) = \sigma_t (A^T A) : (A + A^T)^{-1} (\sigma_t - 2p_t) \quad (37)$$

under the approximation (17). The initial conditions are $m_0 = m_{\text{prior}}$ and $p_0 = 0$, respectively. We note that the differential equations (30) and (37) are explicitly solvable. For example, it holds that

$$\sigma_t = \frac{\sigma_0}{1 + (A^T A) : (A^T + A)^{-1} \sigma_0 t} \quad (38)$$

and one finds that $\sigma_t \sim 1/((A^T A) : (A^T + A)^{-1} t)$ for $t \gg 1$. It can also be shown that $p_t \leq \sigma_t$ for all $t \geq 0$.

We conduct a formal analysis of the ensemble Kalman filter time-stepping (14) and demonstrate that the method is first-order accurate with regard to the implied frequentist mean m_t . We recall (16) and conclude from (14) that the implied update on the variance σ_n satisfies

$$\sigma_{n+1} = \sigma_n - \frac{\sigma_n^2}{\gamma} (A^T A) : C \Delta t + \mathcal{O}(\Delta t^2), \quad (39)$$

which provides a first-order approximation to (30).

We next analyse the evolution equation (28) for the conditional mean μ_t and its numerical approximation

$$\mu_{n+1} = \mu_n + K_n \left\{ (X_{t_{n+1}}^\dagger - X_{t_n}^\dagger) - \mu_n A X_{t_n}^\dagger \Delta t \right\} \quad (40)$$

arising from (14). Here we follow [12] in order to analyse the impact of the data X_t^\dagger on the estimator. An in-depth theoretical treatment can be found in [8].

Comparing (40) to (28) and utilising (16), we find that the key quantity of interest is

$$J_{t_n, t_{n+1}}^\dagger := \int_{t_n}^{t_{n+1}} (A X_t^\dagger)^T dX_t^\dagger, \quad (41)$$

which we can rewrite as

$$J_{t_n, t_{n+1}}^\dagger = A^T : (X_{t_n}^\dagger \otimes X_{t_n, t_{n+1}}^\dagger) + A^T : \mathbb{X}_{t_n, t_{n+1}}^\dagger. \quad (42)$$

Here, motivated by (26) and following standard rough path notation, we have introduced

$$X_{t_n, t_{n+1}}^\dagger := X_{t_{n+1}}^\dagger - X_{t_n}^\dagger \quad (43)$$

and the second-order iterated Itô integral

$$\mathbb{X}_{t_n, t_{n+1}}^\dagger := \int_{t_n}^{t_{n+1}} (X_\tau^\dagger - X_{t_n}^\dagger) \otimes dX_\tau^\dagger. \quad (44)$$

The difference between the integral (41) and its corresponding approximation in (40) is provided by $A^\top : \mathbb{X}_{t_n, t_{n+1}}^\dagger$ plus higher-order terms arising from (16). The iterated integral $\mathbb{X}_{t_n, t_{n+1}}^\dagger$ becomes a random variable from the frequentist perspective. Taking note of (2), we find that the drift $f(x) = Ax$ contributes with terms of order $\mathcal{O}(\Delta t^2)$ to $\mathbb{X}_{t_n, t_{n+1}}^\dagger$ and the expected value of $\mathbb{X}_{t_n, t_{n+1}}^\dagger$ therefore satisfies

$$\mathbb{E}^\dagger[\mathbb{X}_{t_n, t_{n+1}}^\dagger] = \mathcal{O}(\Delta t^2), \quad (45)$$

since

$$\mathbb{E}^\dagger[\mathbb{W}_{t_n, t_{n+1}}^\dagger] = 0, \quad \text{and} \quad \mathbb{E}[W_{t_n, \tau}^\dagger] = 0. \quad (46)$$

Hence we find that, while (40) is not a first-order (strong) approximation of the SDE (28), the approximation becomes first-order in m_t , that is, when averaged over realisations X_t^\dagger of the SDE (2). More precisely, one obtains

$$\mathbb{E}^\dagger[J_{t_n, t_{n+1}}^\dagger] = (A^\top A) : C \Delta t. \quad (47)$$

We note that the modified scheme (24) leads to the same time evolution in the variance σ_n while the update in μ_n is changed to

$$\mu_{n+1} = \mu_n + \frac{\sigma_n}{\gamma} \int_{t_n}^{t_{n+1}} (AX_t^\dagger)^\top dX_t^\dagger - K_n AX_{t_n}^\dagger \mu_n \Delta t. \quad (48)$$

This modification results in a more accurate evolution in the conditional mean μ_n ; but it does not significantly impact on the evolution of the underlying frequentist mean, $m_n = \mathbb{E}^\dagger[\mu_n]$, while leading to an increased computational cost via (25).

In summary, the discrete-time EnKF (14) constitutes a first-order method at the level of the frequentist mean (weak convergence). The frequentist uncertainty is essentially data-independent and only depends on the time window $[0, T]$ over which the data gets observed. Hence, for fixed observation interval $[0, T]$, it makes sense to choose the step-size Δt such that the bias remains on the same order of magnitude as $p_T^{1/2} \approx \sigma_T^{1/2}$. Selecting a much smaller step-size would not reduce the frequentist uncertainty in the conditional estimator μ_T .

Remark 3. We can now also give a precise reformulation of the approximation (23):

$$\frac{1}{2} \mathbb{E}^\dagger \left[A : (X_{t_n, t_{n+1}}^\dagger \otimes X_{t_n, t_{n+1}}^\dagger) \right] = \frac{\Delta t \gamma}{2} \text{tr}(A) + \mathcal{O}(\Delta t^2), \quad (49)$$

which is at the heart of the Stratonovich formulation (19) of the EnKFB [8].

4 Multi-scale data

In this section, we investigate the impact of a possible discrepancy between the SDE model (1), for which we aim to estimate the parameter θ , and the data generating SDE (2). We therefore replace (2) by the the following two-scale SDE [16]:

$$dX_t^{(\epsilon)} = AX_t^{(\epsilon)} dt + \frac{\gamma^{1/2}}{\epsilon} MP_t^{(\epsilon)} dt, \quad (50a)$$

$$dP_t^{(\epsilon)} = -\frac{1}{\epsilon} MP_t^{(\epsilon)} dt + dW_t^\dagger, \quad (50b)$$

where

$$M = \begin{pmatrix} 1 & \beta \\ -\beta & 1 \end{pmatrix}, \quad (51)$$

$\beta = 2$ and $\epsilon = 0.01$. The dimension of state space is $d = 2$ throughout this section. While we restrict here to the simple two-scale model (50), similar scenarios can arise from deterministic fast-slow systems [22, 7].

The associated EnKBF mean-field equations in the parameter Θ_t , which we now denote by $\Theta_t^{(\epsilon)}$ in order to explicitly record its dependence on the scale parameter $\epsilon \ll 1$, become

$$d\Theta_t^{(\epsilon)} = \frac{\sigma_t^{(\epsilon)}}{\gamma} (AX_t^{(\epsilon)})^\top dI_t^{(\epsilon)}, \quad (52a)$$

$$dI_t^{(\epsilon)} = dX_t^{(\epsilon)} - \frac{1}{2} \left(\Theta_t^{(\epsilon)} + \pi_t^{(\epsilon)}[\theta] \right) AX_t^{(\epsilon)} dt, \quad (52b)$$

with variance

$$\sigma_t^{(\epsilon)} = \pi_t^{(\epsilon)} \left[(\theta - \pi_t^{(\epsilon)}[\theta])^2 \right] \quad (53)$$

and $\Theta_t^\epsilon \sim \pi_t^{(\epsilon)}$. The discrete-time mean-field EnKF (14) turns into

$$\Theta_{n+1}^{(\epsilon)} = \Theta_n^{(\epsilon)} + K_n^{(\epsilon)} \left\{ \left(X_{t_{n+1}}^{(\epsilon)} - X_{t_n}^{(\epsilon)} \right) - \frac{1}{2} \left(\Theta_n^{(\epsilon)} + \pi_n^{(\epsilon)}[\theta] \right) AX_{t_n}^{(\epsilon)} \Delta t \right\} \quad (54)$$

with Kalman gain

$$K_n^{(\epsilon)} = \sigma_n^{(\epsilon)} (AX_{t_n}^{(\epsilon)})^\top \left(\gamma + \Delta t \sigma_n^{(\epsilon)} (AX_{t_n}^{(\epsilon)})^\top AX_{t_n}^{(\epsilon)} \right)^{-1}. \quad (55)$$

We also consider the appropriately modified scheme (24):

$$\Theta_{n+1}^{(\epsilon)} = \Theta_n^{(\epsilon)} + \frac{\sigma_n^{(\epsilon)}}{\gamma} \int_{t_n}^{t_{n+1}} (AX_t^{(\epsilon)})^\top dX_t^{(\epsilon)} - \frac{1}{2} K_n^{(\epsilon)} AX_{t_n}^{(\epsilon)} \left(\Theta_n^{(\epsilon)} + \pi_n^{(\epsilon)}[\theta] \right) \Delta t, \quad (56)$$

where again the integral would be approximated using a forward Euler–Maruyama discretisation with internal step-size $\Delta\tau = \Delta t/L \ll \epsilon$.

In order to understand the impact of the modified data generating process on the two mean-field EnKF formulations (54) and (56), respectively, we follow [16] and investigate the difference between $X_t^{(\epsilon)}$ and X_t^\dagger :

$$d(X_t^{(\epsilon)} - X_t^\dagger) = A(X_t^{(\epsilon)} - X_t^\dagger)dt + \frac{\gamma^{1/2}}{\epsilon}MP_t^{(\epsilon)}dt - \gamma^{1/2}dW_t^\dagger \quad (57a)$$

$$= A(X_t^{(\epsilon)} - X_t^\dagger)dt - \gamma^{1/2}dP_t^{(\epsilon)}. \quad (57b)$$

When $P_t^{(\epsilon)}$ is stationary, it is Gaussian with mean zero and covariance

$$\mathbb{E}_{\text{stat}} [P_t^{(\epsilon)} \otimes P_t^{(\epsilon)}] = \epsilon(M + M^T)^{-1} = \frac{\epsilon}{2}I. \quad (58)$$

Hence $P_t^{(\epsilon)} \rightarrow 0$ as $\epsilon \rightarrow 0$ and also

$$X_t^{(\epsilon)} \rightarrow X_t^\dagger \quad (59)$$

in L^2 uniformly in t provided $\sigma(A) \subset \mathbb{C}_-$ and $X_0^{(\epsilon)} = X_0^\dagger$. This is illustrated in Figure 1.

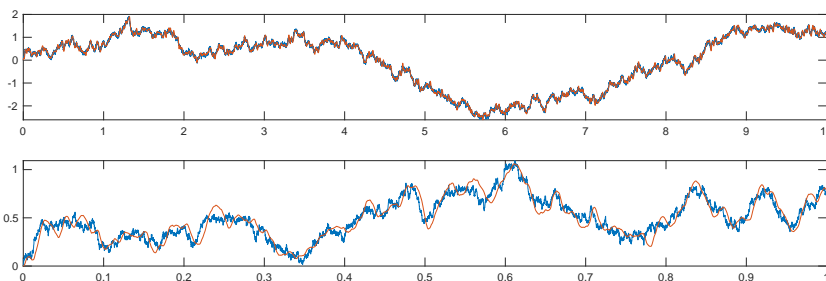


Fig. 1. SDE driven by mathematical vs. physical Brownian motion ($\epsilon = 0.01$). The top panel displays both X_t^\dagger (blue) and $X_t^{(\epsilon)}$ (red) over the long time interval $t \in [0, 10]$, while the lower panel provides a zoomed in perspective over the interval $t \in [0, 1]$.

In order to investigate the problem further, we study the integral

$$J_{t_n, t_{n+1}}^{(\epsilon)} := \int_{t_n}^{t_{n+1}} (AX_t^{(\epsilon)})^T dX_t^{(\epsilon)} \quad (60)$$

and its relation to (41). As for (41), we can rewrite (60) as

$$J_{t_n, t_{n+1}}^{(\epsilon)} = A^T : (X_{t_n}^{(\epsilon)} \otimes X_{t_n, t_{n+1}}^{(\epsilon)}) + A^T : \mathbb{X}_{t_n, t_{n+1}}^{(\epsilon)}. \quad (61)$$

We now determine the second-order iterated integral $\mathbb{X}_{t_n, t_{n+1}}^{(\epsilon)}$ in the limit $\epsilon \rightarrow 0$ [16]:

$$\mathbb{X}_{t_n, t_{n+1}}^{(\epsilon)} = \int_{t_n}^{t_{n+1}} X_{t_n, t}^{(\epsilon)} \otimes dX_t^{(\epsilon)} \quad (62a)$$

$$\rightarrow \int_{t_n}^{t_{n+1}} X_{t_n,t}^\dagger \otimes dX_t^\dagger - \gamma^{1/2} \int_{t_n}^{t_{n+1}} X_{t_n,t}^{(\epsilon)} \otimes dP_t^{(\epsilon)} \quad (62b)$$

$$= \mathbb{X}_{t_n,t_{n+1}}^\dagger - \gamma^{1/2} X_{t_n,t_{n+1}}^{(\epsilon)} \otimes P_{t_{n+1}}^{(\epsilon)} + \gamma^{1/2} \int_{t_n}^{t_{n+1}} dX_t^{(\epsilon)} \otimes P_t^{(\epsilon)} \quad (62c)$$

$$\rightarrow \mathbb{X}_{t_n,t_{n+1}}^\dagger + \gamma^{1/2} \int_{t_n}^{t_{n+1}} \left\{ AX_t^{(\epsilon)} + \frac{\gamma^{1/2}}{\epsilon} MP_t^{(\epsilon)} \right\} \otimes P_t^{(\epsilon)} dt \quad (62d)$$

$$\rightarrow \mathbb{X}_{t_n,t_{n+1}}^\dagger + \frac{\Delta t \gamma}{\epsilon} M \mathbb{E}_{\text{stat}} \left[P_{t_n}^{(\epsilon)} \otimes P_{t_n}^{(\epsilon)} \right] \quad (62e)$$

$$= \mathbb{X}_{t_n,t_{n+1}}^\dagger + \frac{\Delta t \gamma}{2} M. \quad (62f)$$

Hence we may conclude that the discrete-time EnKF (54) converges to (14) for fixed Δt as $\epsilon \rightarrow 0$. This has been verified numerically in [24] already. On the other hand, as discussed in detail in [8], the same is not true for the associated schemes (24) and (56), respectively, since

$$J_{t_n,t_{n+1}}^\dagger = \lim_{\epsilon \rightarrow 0} J_{t_n,t_{n+1}}^{(\epsilon)} - \frac{\Delta t \gamma}{2} A^T : M. \quad (63)$$

This observation suggests the following modification

$$\Theta_{n+1}^{(\epsilon)} = \Theta_n^{(\epsilon)} + \frac{\sigma_n^{(\epsilon)}}{\gamma} \int_{t_n}^{t_{n+1}} (AX_t^{(\epsilon)})^T dX_t^{(\epsilon)} - \frac{\Delta t}{2} \sigma_n^{(\epsilon)} A^T : M - \quad (64a)$$

$$\frac{1}{2} K_n^{(\epsilon)} AX_{t_n}^{(\epsilon)} \left(\Theta_n^{(\epsilon)} + \pi_n^{(\epsilon)}[\theta] \right) \Delta t \quad (64b)$$

to (56).

If M in (63) is unknown, an appropriate estimator is required. While the estimator proposed in [8] is based on the idea of subsampling the data, the frequentist perspective taken in this note suggests the alternative estimator M_{est} defined by

$$\frac{\Delta t \gamma}{2} M_{\text{est}} = \mathbb{E}^\dagger [\mathbb{X}_{t_n,t_{n+1}}^{(\epsilon)}], \quad (65)$$

which follows from (62f) and (45), that is, $\mathbb{E}^\dagger [\mathbb{X}_{t_n,t_{n+1}}^\dagger] = \mathcal{O}(\Delta t^2)$ for Δt sufficiently small. In practice, the frequentist expectation value can be replaced by an approximation along a given single observation path $X_t^{(\epsilon)}$, $t \in [0, T]$, under the assumption of ergodicity.

An appropriate choice of the outer or sub-sampling step-size Δt [25] constitutes another important aspect for the practical implementation of the EnKF formulation (54) for finite values of $\epsilon > 0$ [24]. Consistency of the second-order iterated integrals [12] implies

$$\mathbb{X}_{t_n,t_{n+2}}^{(\epsilon)} = \mathbb{X}_{t_n,t_{n+1}}^{(\epsilon)} + \mathbb{X}_{t_{n+1},t_{n+2}}^{(\epsilon)} + X_{t_n,t_{n+1}}^{(\epsilon)} \otimes X_{t_{n+1},t_{n+2}}^{(\epsilon)}. \quad (66)$$

A sensible choice of Δt is dictated by

$$\mathbb{E}^\dagger \left[X_{t_n,t_{n+1}}^{(\epsilon)} \otimes X_{t_{n+1},t_{n+2}}^{(\epsilon)} \right] = \mathcal{O}(\Delta t^2), \quad (67)$$

that is, the sub-sampled data $X_{t_n}^{(\epsilon)}$ behaves to leading order like solution increments from the reference model (2) at scale Δt independent of the specific value of ϵ . Note that, on the other hand,

$$\mathbb{E}^\dagger \left[X_{\tau_l, \tau_{l+1}}^{(\epsilon)} \otimes X_{\tau_{l+1}, \tau_{l+2}}^{(\epsilon)} \right] = \mathcal{O}(\epsilon^{-1} \Delta \tau^2) \quad (68)$$

for an inner step-size $\Delta \tau \sim \epsilon$. In other words, a suitable step-size $\Delta t > 0$ can be defined by making

$$h(\Delta t) := \Delta t^{-2} \left\| \mathbb{E}^\dagger \left[X_{t_n, t_{n+1}}^{(\epsilon)} \otimes X_{t_{n+1}, t_{n+2}}^{(\epsilon)} \right] \right\| \quad (69)$$

as small as possible while still guaranteeing an accurate numerical approximation in (54).

Remark 4. The choice of the outer time step Δt is less critical for the EnKF formulation (64) since it does not rely on sub-sampling the data and is robust with regard to perturbations in the data. Furthermore, if either $\beta = 0$ in (51) or A is symmetric, then one can use the approximation

$$\begin{aligned} \int_{t_n}^{t_{n+1}} (AX_t^{(\epsilon)})^\top dX_t^{(\epsilon)} &\approx A : \left(X_{t_n}^{(\epsilon)} \otimes X_{t_n, t_{n+1}}^{(\epsilon)} + \frac{1}{2} X_{t_n, t_{n+1}}^{(\epsilon)} \otimes X_{t_n, t_{n+1}}^{(\epsilon)} \right) \quad (70a) \\ &= A : X_{t_{n+1/2}}^{(\epsilon)} \otimes X_{t_n, t_{n+1}}^{(\epsilon)} \quad (70b) \end{aligned}$$

in (64). This insight is at the heart of the geometric rough path approach followed in [8] and which starts from the Stratonovich formulation (19) of the EnKBF. See also [26] on the convergence of Wong–Zakai approximations for stochastic differential equations. In all other cases, a more refined numerical approximation of the data-driven integral in (64) is necessary; such as, for example, (25). For that reason, we rely on the Itô/Euler–Maruyama interpretation of (60) in this note instead; that is approximation (7).

5 Numerical example

We consider the linear SDE (2) with $\gamma = 1$ and

$$A = \frac{-1}{2} \begin{pmatrix} 1 & -1 \\ 1 & 1 \end{pmatrix}. \quad (71)$$

We find that $C = I$ and $A^\top A = 1/2I$. Hence $(A^\top A) : C = 1$ and the posterior variance simply satisfies $\sigma_t = \sigma_0 / (1 + \sigma_0 t)$ according to (38). We set $m_{\text{prior}} = 0$ and $\sigma_{\text{prior}} = 4$ for the Gaussian prior distribution of Θ_0 and the observation interval is $[0, T]$ with $T = 6$. We find that $\sigma_T = 0.16$. Solving (33) for given σ_t with initial condition $m_0 = 0$ yields

$$m_t = 1 - \frac{\sigma_t}{\sigma_0} \quad (72)$$

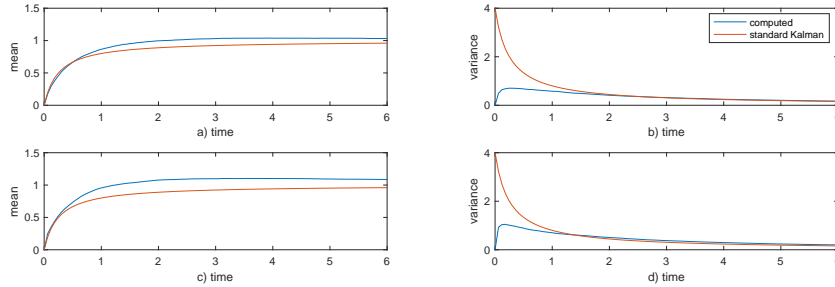


Fig. 2. a)–b): frequentist mean, m_t and variance, p_t , from EnKF implementation (14) with step-size $\Delta t = 0.06$; c)–d): same results from EnKF implementation (24) with inner time-step $\Delta\tau = \Delta t/600$. We also display the curves arising for σ_t and m_t from the standard Kalman theory using the approximation (17). Note that the posterior variance, σ_t , should provide an upper bound on the frequentist uncertainty p_t .

and $m_T = 0.96$. The corresponding curves are displayed in red in Figure 2.

We implement the EnKF schemes (14) and (24) with $t_n = n \Delta t$. The inner time-step is $\Delta\tau = 10^{-4}$ while $\Delta t = 0.06$, that is, $L = 600$. We repeat all the experiment $N = 10^4$ times and compare the outcome with the predicted mean value of $m_T = 0.96$ and the posterior variance of $\sigma_T = 0.16$ in Figure 2. The differences in the computed time evolutions of m_t and p_t are rather minor and support the idea that it is not necessary to assimilate continuous-time data beyond Δt . We also find that the simple prediction (72), based on standard Kalman filter theory, is not very accurate for this low-dimensional problem ($d = 2$). The corresponding approximation for σ_t provides however a good upper bound for p_t .

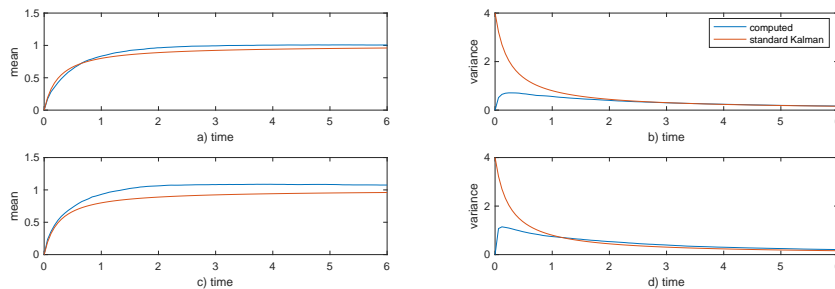


Fig. 3. Same experimental setting as in Figure 2 but with the data now generated from the multi-scale SDE (50). Again, subsampling the data in intervals of $\Delta t = 0.06$ and high-frequency assimilation with step-size $\Delta\tau = 10^{-4}$ lead to very similar results in terms of their frequentist means and variances.

We now replace the data generating SDE model (2) by the multi-scale formulation (50) with $\epsilon = 0.01$ and $\beta = 2$. This parameter choice agrees with the one used in [8]. We again find that assimilating the data at the slow time-scale $\Delta t = 0.06$ leads to very similar results obtained from an assimilation at the fast time-scale $\Delta \tau = 10^{-4}$ with the EnKF formulation (64) provided the correction term resulting from the second-order iterated integral (63) is included. We also verified numerically that $\Delta t = 0.06$ constitutes a nearly optimal step-size in the sense of making (69) sufficiently small while maintaining numerical accuracy. For example, reducing the outer step-size to $\Delta t = 0.02$ leads to $h(0.02) - h(0.06) \approx 10$ in (69).

6 Conclusions

In this follow-up note to [8], we have investigated the impact of subsampling and/or high-frequency data assimilation on the corresponding conditional mean estimators, μ_t , both for data generated from the standard SDE model and a modified multi-scale SDE. A frequentist analysis supports the basic finding that both approaches lead to comparable results provided systematic biases due to different second-order iterated integrals are properly accounted for. While the EnKBF is relatively easy to analyse and a full rough path approach can be avoided, extending these results to the nonlinear feedback particle filter [24, 8] will prove more challenging. Extensions to systems without a strong scale separation [4, 28] and applications to geophysical fluid dynamics [20, 11] are also of interest. In this context, the approximation quality of the proposed estimator (65) and the choice of the step-size Δt following (69) (and potentially $\Delta \tau$) will be of particular interest. Finally, while we have investigated the univariate parameter estimation problem, a semi-parametric parametrisation of the drift term f in (1), such as random feature maps [19], lead to high-dimensional parameter estimation problems and their statistics [17, 18], which provides another fertile direction for future research.

Acknowledgements. SR has been partially funded by Deutsche Forschungsgemeinschaft (DFG) - Project-ID 318763901 - SFB1294 and Project-ID 235221301 - SFB1114. He would also like to thank Nikolas Nüsken for many fruitful discussions on the subject of this paper.

Bibliography

- [1] A. Abdulle, G. Garegnani, G. A. Pavliotis, A. M. Stuart, and A. Zaroni. Drift estimation of multiscale diffusions based on filtered data. *Foundations of Computational Mathematics*, published online 2021/10/13:in press, 2021. doi: 10.1007/s10208-021-09541-9.
- [2] Y. Ait-Sahalia, P. A. Mykland, and L. Zhang. How often to sample a continuous-time process in the presence of market microstructure noise. *The Review of Financial Studies*, 18:351–416, 2005.
- [3] J. Amezcua, E. Kalnay, K. Ide, and S. Reich. Ensemble transform Kalman-Bucy filters. *Q.J.R. Meteor. Soc.*, 140:995–1004, 2014.
- [4] L. Arnold. Hasselmann’s program revisited: The analysis of stochasticity in deterministic climate models. In *Stochastic Climate Models*, pages 141–158. Birkhäuser Basel, 2001. doi: 10.1007/978-3-0348-8287-3.
- [5] R. Azencott, A. Beri, A. Jain, and I. Timofeyev. Sub-sampling and parametric estimation for multiscale dynamics. *Communications in Mathematical Sciences*, 11:939–970, 2013.
- [6] A. Bain and D. Crisan. *Fundamentals of Stochastic Filtering*, volume 60 of *Stoch. Model. Appl. Probab.* Springer, New York, 2009. doi: 10.1007/978-0-387-76896-0.
- [7] P. Bálint and I. Melbourne. Statistical properties for flows with unbounded roof function, including the Lorenz attractor. *Journal of Statistical Physics*, 172:1101–1126, 2018. doi: 10.1007/s10955-018-2093-y.
- [8] M. Coghi, T. Nilssen, N. Nüsken, and S. Reich. Rough McKean–Vlasov dynamics for robust ensemble Kalman filtering, 2021. arXiv:2107.06621.
- [9] C. Cotter and S. Reich. Ensemble filter techniques for intermittent data assimilation. *Radon Ser. Comput. Appl. Math.*, 13:91–134, 2013. doi: 10.1515/9783110282269.91.
- [10] D. Crisan, J. Diehl, P. K. Friz, H. Oberhauser, et al. Robust filtering: correlated noise and multidimensional observation. *The Annals of Applied Probability*, 23:2139–2160, 2013.
- [11] J. Culina, S. Kravtsov, and A. H. Monahan. Stochastic parameterization schemes for use in realistic climate models. *Journal of the Atmospheric Sciences*, 68:284 – 299, 2011. doi: 10.1175/2010JAS3509.1.
- [12] A. M. Davie. Differential equations driven by rough paths: an approach via discrete approximation. *Applied Mathematics Research eXpress*, 2008, 2008. doi: 10.1093/amrx/abm009. abm009.
- [13] J. Diehl, P. Friz, and H. Mai. Pathwise stability of likelihood estimators for diffusion via rough paths. *The Annals of Applied Probability*, 26:2169–2192, 2016. doi: 10.1214/15-AAP1143.
- [14] G. Evensen. *Data assimilation*. Springer-Verlag, Berlin, second edition, 2009. ISBN 978-3-642-03710-8. doi: 10.1007/978-3-642-03711-5.
- [15] P. Friz and M. Hairer. *A course on rough paths*. Springer-Verlag, 2020.

- [16] P. Friz, P. Gassiat, and T. Lyons. Physical Brownian motion in a magnetic field as a rough path. *Transactions of the American Mathematical Society*, 367:7939–7955, 2015.
- [17] S. Ghosal and A. van der Vaart. *Fundamentals of Nonparametric Bayesian Inference*. Cambridge Series in Statistical and Probabilistic Mathematics. Cambridge University Press, 2017. doi: 10.1017/9781139029834.
- [18] E. Giné and R. Nickl. *Mathematical Foundations of Infinite-Dimensional Statistical Models*. Cambridge University Press, Cambridge, 2016. doi: 10.1017/CBO9781107337862.
- [19] G. A. Gottwald and S. Reich. Supervised learning from noisy observations: Combining machine-learning techniques with data assimilation. *Physica D: Nonlinear Phenomena*, 423:132911, 2021. ISSN 0167-2789. doi: <https://doi.org/10.1016/j.physd.2021.132911>.
- [20] K. Hasselmann. Stochastic climate models Part I. Theory. *Tellus*, 28:473–485, 1976. doi: 10.1111/j.2153-3490.1976.tb00696.x.
- [21] N. Ikeda and S. Watanabe. *Stochastic differential equations and diffusion processes*. North Holland Publishing Company, Amsterdam-New York, 2nd edition, 1989.
- [22] D. Kelly and I. Melbourne. Deterministic homogenization for fast-slow systems with chaotic noise. *Journal of Functional Analysis*, 272:4063–4102, 2017. doi: 10.1016/j.jfa.2017.01.015.
- [23] Y. A. Kutoyants. *Statistical inference for ergodic diffusion processes*. Springer Science & Business Media, 2013.
- [24] N. Nüsken, S. Reich, and P. J. Rozdeba. State and parameter estimation from observed signal increments. *Entropy*, 21(5):505, 2019. doi: 10.3390/e21050505.
- [25] A. Papavasiliou, G. Pavliotis, and A. Stuart. Maximum likelihood estimation for multiscale diffusions. *Stochastic Processes and their Applications*, 19:3173–3210, 2009.
- [26] S. Pathiraja. L^2 convergence of smooth approximations of stochastic differential equations with unbounded coefficients, 2020. arXiv:2011.13009.
- [27] S. Reich and P. Rozdeba. Posterior contraction rates for non-parametric state and drift estimation. *Foundation of Data Science*, 2:333–349, 2020. doi: 10.3934/fods.2020016.
- [28] J. Wouters and G. A. Gottwald. Stochastic model reduction for slow-fast systems with moderate time scale separation. *Multiscale Modeling & Simulation*, 17:1172–1188, 2019.